Dynamics and bifurcation analysis of the heat-shock response in eukaryotic cells

DYNAMICS AND BIFURCATION ANALYSIS OF THE HEAT-SHOCK RESPONSE IN EUKARYOTIC CELLS

Dimitrios I. Gerogiorgis
Department of Chemical Engineering, Massachusetts Institute of Technology, MA 02139, USA

Abstract

The heat-shock response mechanism in eukaryotic cells is one of the most important survival features of living organisms and comprises a genetic network coordinating the cellular response to protein damage. The importance and function of the heat-shock transcription factor-1 (HSF-1), which is central to the heat-shock response mechanism, has been studied extensively, as documented in numerous publications. Detailed network representations and dynamic mathematical models have been derived and tested in order to analyze quantitatively all species and their concentrations in the heat-shock response cycle. Furthermore, parameter estimation and sensitivity analysis have provided additional insight regarding the relative importance of a large number of kinetic parameters within the respective expression networks. This paper focuses on analyzing the importance of an uncertain, temperature-dependent parameter ($\beta_{m,k}$). A bifurcation analysis is conducted in order to identify and analyze multiple steady states of the system.

Keywords

Heat-shock response, heat-shock factor (HSF), heat-shock protein (HSP), modeling, bifurcation analysis.

Introduction

The *heat-shock response mechanism* in eukaryotic cells (Lindquist, 1986) is an adaptation and survival reaction against the proteotoxicity resulting from the appearance of many classes of non-native (misfolded, damaged) proteins. The accumulation of such non-native protein species can result in the dangerous generation of protein aggregates. To handle this build-up of abnormal proteins, cells employ a complicated machinery of *molecular chaperones*: these species facilitate the refolding or degradation of misfolded polypeptides, prevent protein aggregation and play a role in formation of aggresome, a centrosome-associated body to which small cytoplasmic aggregates are transported. Protein folding and toxic aggregates have been studied in the domain of neurochemistry and molecular neurobiology (even though mathematical modeling is very cumbersome), and they are increasingly recognized as responsible for the progression of serious neurodegenerative diseases, which have a severe impact on progressively larger populations. These include Alzheimer's, Parkinson's and Huntington's diseases, and Amyotrophic Lateral Sclerosis; all are quite common (Meriin & Sherman, 2005; Szilágyi et al., 2007).

Heat-shock proteins (HSPs) are vital regulatory elements which act as molecular chaperones: upon sensing stress signals (elevated temperatures, toxic molecules, oxidants, heavy metals), cells resort to transient molecular chaperone overexpression, to meet the stress demand by high levels. Thus, they ensure protein quality control and homeostasis. Chaperones recognize exposed hydrophobic patches on unfolded polypeptides and sequester them until they reach their native conformation by proper refolding, or escort proteosomes to degradation (Muchowski & Wacker, 2005). They also have documented effects, via hitherto unknown mechanisms, in tumour cell apoptosis (Creagh et al., 2000). The conceptual biomolecular model of Morimoto (1993) and his experimental studies (Kline & Morimoto, 1997) identified the key elementary steps of heat-shock response. Rieger et al. (2005) provided *the first mathematical model of HSF regulation* with predictive capability, establishing systematically the most sensitive steps of the mechanism. Rigorous investigation of multiple system steady states and possible bifurcation effects have not been pursued so far, and this is the main objective of the present research study.

Literature Review

Morimoto proposed the HSF regulation model (1993). In unstressed cells, HSF is maintained in a monomeric, non-DNA binding form via its interactions with hsp70 (1). Upon heat shock, HSF undergoes rapid homotrimerization (2), binding to a heat-shock DNA element (HSE) (3), and phosphorylation (4). Transcriptional activation due to heat shock genes leads to hsp70 overexpression and formation of an HSF-hsp70 complex (5). Finally, HSF dissociates from DNA, converted to non-DNA-binding monomers (6).

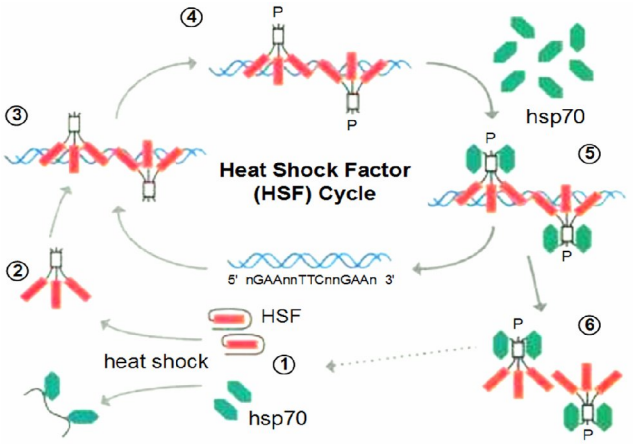

Figure 1. The model of HSF regulation (Morimoto, 1993).

Rieger et al. (2005) presented a detailed model of HSP expression and regulation: the heat shock (ΔT) switches a stress-dependent kinase from its inactive (S) to active form (S^*), and the latter is deactivated by dephosphorylation (2). The transcription factor (HSF) binds to the DNA site (3), where it is bound by S^* (4) and phosphorylated to its active form (5); that induces transcription (6) and translation (7). HSP binds to the active form, repressing transcription (8). This latter inactive form is also subject to binding (9) and dephosphorylation (10) by deactivating phosphatase (I). HSP also binds HSF on HSE before phosphorylation (11), but also sequesters HSF in solution, off DNA sites (12-13). The mRNA is assumed to be stabilized by S^* (14); also, mRNA and HSP are subject to first-order decay (15–16). A larger model has also appeared lately (Petre et al., 2008).

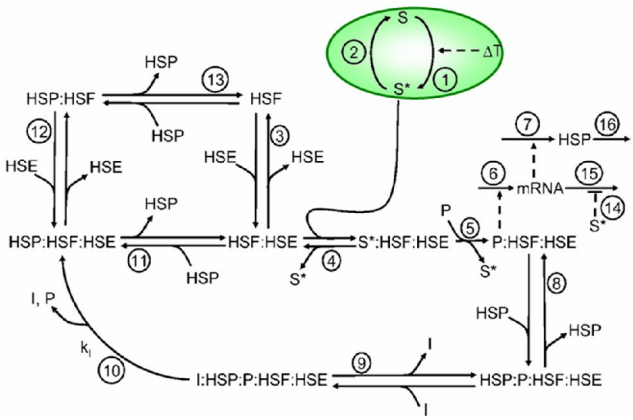

Figure 2. The detailed kinetic model (Rieger et al., 2005).

Mathematical Modeling

The key biomolecular species and the corresponding concentration variables of the model are listed in Table 1.

Table 1: Key model species and concentration variables.

Species	Desciption	Variable
HSF	Free HSF1	(x_1)
HSE	Free promoter site on the DNA	(x_2)
HSF:HSE	Inactive HSF1 bound to promoter site	(x_3)
S^*:HSF:HSE	Active kinase bound to HSF on DNA site	(x_4)
P:HSF:HSE	Phosphorylated HSF1 on the DNA site	(x_5)
HSP:P:HSF:HSE	HSP bound to phosph. HSF1 on DNA site	(x_6)
I:HSP:P:HSF:HSE	Phosphatase on phosph. complex on DNA site	(x_7)
HSP:HSF:HSE	HSP bound to unphosph. HSF1 on DNA site	(x_8)
HSP:HSF	HSP bound to HSF off the DNA site	(x_9)
mRNA	Chaperone mRNA	(x_{10})
HSP	Free, unbound heat-shock protein	(x_{11})
S*	Free, unbound active stress kinase	(x_{12})
I	Free, unbound stress phosphatase	(x_{13})
S	Free, unbound inactive stress kinase	(algebraic)
P	Free phosphate (assumed in excess)	(–)

The model includes 13 ordinary differential equations and 27 parameters, which are presented in Tables 2 and 3.

Table 2: The complete dynamic model (Rieger et al., 2005).

$$\frac{dx_1}{d\tau} = \frac{\kappa_1}{\rho_E}\left(x_3 - \Gamma_1 x_1 x_2\right) + \kappa_7\left(x_9 - \Gamma_7 x_1 x_{11}\right) \quad (1)$$

$$\frac{dx_2}{d\tau} = \kappa_1\left(x_3 - \Gamma_1 x_1 x_2\right) + \kappa_6\left(x_8 - \Gamma_6 x_2 x_9\right) \quad (2)$$

$$\frac{dx_3}{d\tau} = \kappa_1\left(\Gamma_1 x_1 x_2 - x_3\right) + \kappa_2\left(x_4 - \Gamma_2 x_3 x_{12}\right) + \kappa_5\left(x_8 - \Gamma_5 x_3 x_{11}\right) \quad (3)$$

$$\frac{dx_4}{d\tau} = \kappa_2\left(\Gamma_2 x_3 x_{12} - x_4\right) - \kappa_S x_4 \quad (4)$$

$$\frac{dx_5}{d\tau} = \kappa_S x_4 + \kappa_3\left(x_6 - \Gamma_3 x_5 x_{11}\right) \quad (5)$$

$$\frac{dx_6}{d\tau} = \kappa_3\left(\Gamma_3 x_5 x_{11} - x_6\right) + \kappa_4\left(x_7 - \Gamma_4 x_6 x_{13}\right) \quad (6)$$

$$\frac{dx_7}{d\tau} = \kappa_4\left(\Gamma_4 x_6 x_{13} - x_7\right) - \kappa_1 x_7 \quad (7)$$

$$\frac{dx_8}{d\tau} = \kappa_1 x_7 + \kappa_5\left(\Gamma_5 x_3 x_{11} - x_8\right) + \kappa_6\left(\Gamma_6 x_2 x_9 - x_8\right) \quad (8)$$

$$\frac{dx_9}{d\tau} = \frac{\kappa_6}{\rho_E}\left(x_8 - \Gamma_6 x_2 x_9\right) + \kappa_7\left(\Gamma_7 x_1 x_{11} - x_9\right) \quad (9)$$

$$\frac{dx_{10}}{d\tau} = \kappa_{tr} x_5 - \frac{\Gamma_S}{\Gamma_S + \rho_S x_{12}} x_{10} \quad (10)$$

$$\frac{dx_{11}}{d\tau} = \kappa_{tr} x_{10} - \kappa_{d,p} x_{11} + \kappa_3\left(x_6 - \Gamma_3 x_5 x_{11}\right) + \kappa_5\left(x_8 - \Gamma_5 x_3 x_{11}\right) + \kappa_7 \rho_E\left(x_9 - \Gamma_7 x_1 x_{11}\right) \quad (11)$$

$$\frac{dx_{12}}{d\tau} = \beta_{m,k}\frac{\left(1 - \frac{x_4}{\rho_S} - x_{12}\right)}{\Gamma_{m,k} + \left(1 - \frac{x_4}{\rho_S} - x_{12}\right)} - \beta_{m,p}\frac{x_{12}}{\Gamma_{m,p} + x_{12}} + \frac{\kappa_2}{\rho_S}\left(x_4 - \Gamma_2 x_3 x_{12}\right) + \frac{\kappa_S}{\rho_S} x_4 \quad (12)$$

$$\frac{dx_{13}}{d\tau} = \frac{\kappa_4}{\rho_I}\left(x_7 - \Gamma_4 x_6 x_{13}\right) + \frac{\kappa_I}{\rho_I} x_7 \quad (13)$$

$$HSF_{tb} = x_3 + x_4 + x_5 + x_6 + x_7 + x_8 \quad (14)$$

$$HSF_p = x_5 + x_6 + x_7 \quad (15)$$

$$HSP_{tr} = \kappa_{tr} x_5 \quad (16)$$

Table 3: Dimensionless parameters and numerical values.

Symbol	Value	Step (Fig. 2)	Symbol	Value	Step (Fig. 2)
$\boldsymbol{\beta_{m,k}}$	varies	bif. parameter	κ_1	$6.0\cdot10^{1}$	(10)
$\Gamma_{m,k}$	$5.0\cdot10^{-2}$	(1)	Γ_1	$3.0\cdot10^{-3}$	(3)
$\beta_{m,p}$	$1.0\cdot10^{3}$	(2)	Γ_2	$5.0\cdot10^{1}$	(4)
$\Gamma_{m,p}$	$5.0\cdot10^{-2}$	(2)	Γ_3	$5.0\cdot10^{-3}$	(8)
κ_1	$9.8\cdot10^{5}$	(3)	Γ_4	$5.0\cdot10^{0}$	(9)
κ_2	$3.0\cdot10^{3}$	(4)	Γ_5	$1.0\cdot10^{-3}$	(11)
κ_3	$5.9\cdot10^{5}$	(8)	Γ_6	$5.0\cdot10^{-4}$	(12)
κ_4	$3.0\cdot10^{3}$	(9)	Γ_7	$7.5\cdot10^{-2}$	(13)
κ_5	$3.0\cdot10^{6}$	(11)	Γ_S	$2.0\cdot10^{-1}$	(14)
κ_6	$5.9\cdot10^{6}$	(12)	$\kappa_{d,p}$	$3.0\cdot10^{-3}$	(15-16)
κ_7	$4.0\cdot10^{4}$	(13)	ρ_E	$1.0\cdot10^{2}$	(scaling)
κ_S	$3.0\cdot10^{2}$	(5)	ρ_S	$1.0\cdot10^{4}$	(scaling)
κ_{tr}	$1.2\cdot10^{1}$	(6)	ρ_I	$1.0\cdot10^{0}$	(scaling)
κ_{ta}	$1.2\cdot10^{1}$	(7)	τ	Dimensionless time, t/τ^*	

Dynamic Simulation

Dynamic simulation via the ODE model (Table 2) clearly illustrates the critical effect of parameter $\beta_{m,k}$ on the concentration of free hsp70 as well as on system stability (x_5/pink-x_{11}/red are indicators of transcriptional activation). Figures 3 and 4 illustrate clearly different x_i responses for $\beta_{m,k}$ values corresponding to 37 and 41 °C, respectively. The initial condition (IC) vector that has been used in both dynamic simulations is: $\boldsymbol{x}_{IC} = [1\ 1\ 0\ 0\ 0\ 0\ 0\ 0\ 0\ 0\ 0\ 1\ 1]^T$.

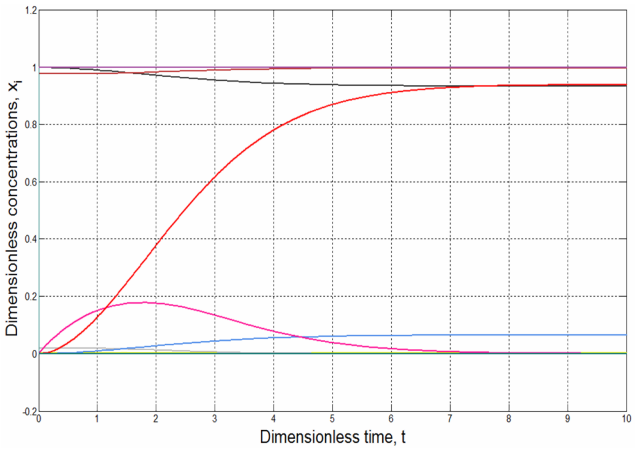

Figure 3. Dynamic simulation of a bounded x_{11} response.

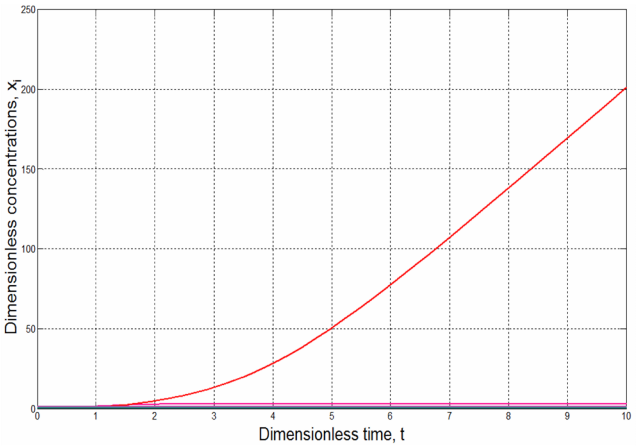

Figure 4. Dynamic simulation of a divergent x_{11} response.

Phase Plane Analysis

Phase plane analysis of the heat-shock dynamic model provides visual insight for understanding its intricacies. This nonlinear ODE model exhibits multiple steady states, which have not been discussed or documented previously. A trivial steady state is: $\boldsymbol{x}^{0}_{ss} = [0\ 0\ 0\ 0\ 0\ 0\ 0\ 0\ 0\ 0\ 0\ \rho^*_{12}\ 0]^T$. Besides the finite equilibrium points, the 21 bilinear terms (7 distinct bilinearities $x_i x_j$, each occurring 3 times therein) produce *equilibrium sets*, some observable by inspection. Only variables x_1, x_2, x_{13} occur exclusively in bilinear terms (coupled to x_6, x_9, x_{11}) and thus affect equilibria indirectly. One obvious set is $\boldsymbol{x}^{I}_{ss} = [p_1\ 0\ 0\ 0\ 0\ 0\ 0\ 0\ 0\ 0\ 0\ \rho^*_{12}\ p_{13}]^T$; another such set is $\boldsymbol{x}^{II}_{ss} = [0\ p_2\ 0\ 0\ 0\ 0\ 0\ 0\ 0\ 0\ 0\ \rho^*_{12}\ p_{13}]^T$ ($\rho^*_{12} = 2.8571\cdot10^{-7}$ is a distinct root, $p_i \in \Re_+$ are parameters). Figure 5 shows the convergence of x_{12} to ρ^*_{12} for $x_{5,0} \in \Re_+$.

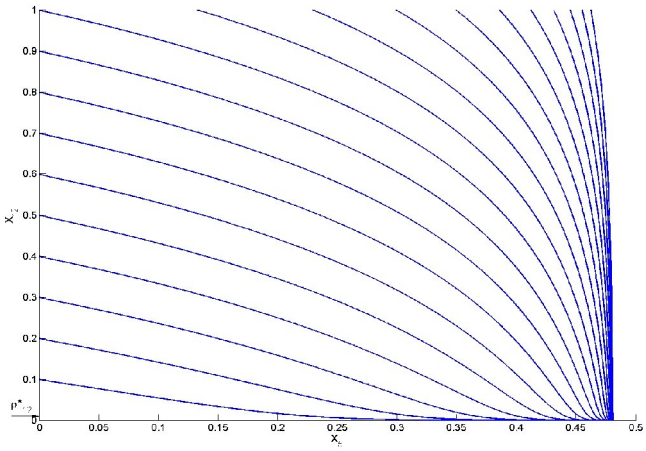

Figure 5. Phase plot: convergence in x_5-x_{12} subspace.

Trivial sets do not portray realistic intracellular action, but show that the stationary nonlinear algebraic system ($\dot{\boldsymbol{x}} = 0$) may admit an infinite number of solutions, as prescribed by a generalized Bézout Theorem (Allgower & Georg, 1990). A *biologically relevant system mode* and its equilibrium set are discovered by continuously varying parameter $\beta_{m,k}$, with $\boldsymbol{x}^*_{IC} = [p^*\ p^*\ ..\ p^*]^T$ ($p^* = 0.05$), as presented in Figure 6.

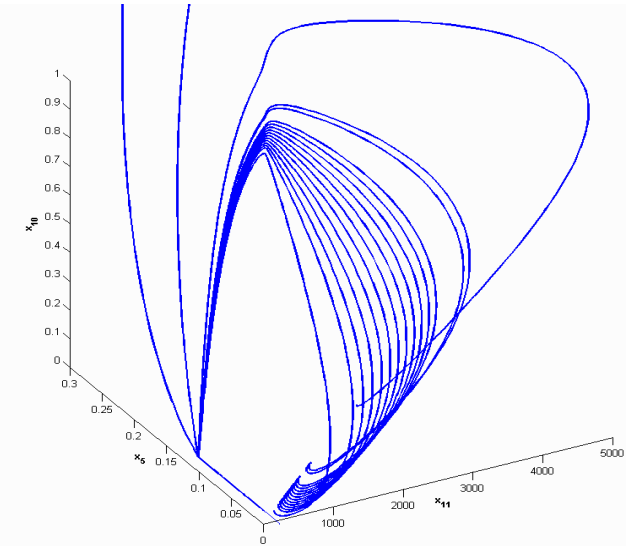

Figure 6. Phase plot: $\beta_{m,k}$ variation in x_5-x_{10}-x_{11} subspace.

Bifurcation Analysis

Our research goal is to perform a bifurcation analysis on the heat-shock dynamic model in order to understand the hitherto unexplored effect of $\beta_{m,k}$ on system responses for a multitude of biologically relevant equilibrium points. Figure 6 reveals a notable mode in the x_5-x_{10}-x_{11} subspace: considering computations initiated from $\boldsymbol{x}^*_{IC} = [p^* p^* .. p^*]^T$, low-$\beta_{m,k}$ trajectories reach a maximum and converge back close to the x_5-x_{10} plane, but high-$\beta_{m,k}$ trajectories attain high x_{10} and extreme x_{11} equilibrium values, despite scaling.

As $\beta_{m,k}$ is temperature-dependent and corresponds to the equilibrium constant of S activation (Fig. 2, steps 1-2), its value spans 7 orders of magnitude (Rieger et al., 2005), from $\beta_{m,k}$ (T=37 °C) = $6.0 \cdot 10^{-3}$ to $\beta_{m,k}$ (T=43 °C) = $1.0 \cdot 10^{4}$. A critical value ($\beta^*_{m,k}$) triggering transition (Seydel, 1994) may signify the onset of irreversible biological damage (recovery is observed experimentally for limited exposure). Special bifurcation analysis software (MATCONT® v. 2.4.2) has been employed here to explore the important subspace elements vs. $\beta_{m,k}$ and determine $\beta^*_{m,k}$ (Dhooge et al., 2003).

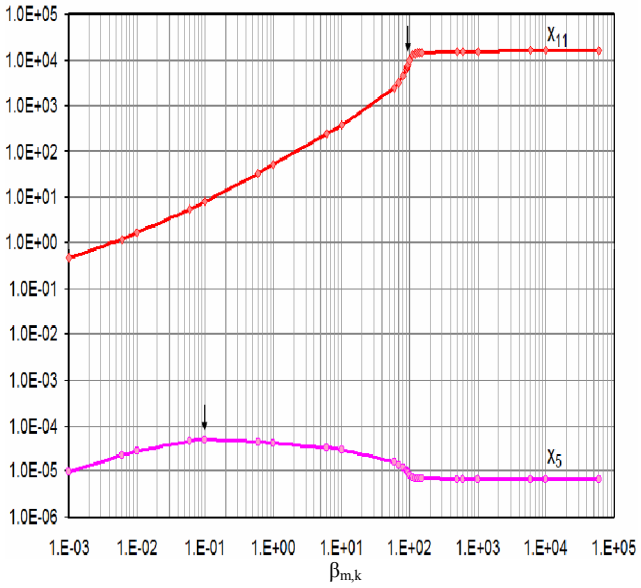

Figure 7. Bifurcation diagram: x_5, x_{11} steady states vs. $\beta_{m,k}$.

An exponential correlation has been used to model the nonlinear dependence of $\beta_{m,k}$ on temperature, and estimate the temperature corresponding to the critical value ($\beta^*_{m,k}$). Table 4 shows the nonlinear fit and critical point obtained.

Table 4: Parameter $\beta_{m,k}$ value as a function of temperature.

T (°C)	37	**39.21**	41	42	43
T (K)	310.15	**312.36**	314.15	315.15	316.15
$\beta_{m,k}$	$6.0 \cdot 10^{-3}$	$\mathbf{9.2 \cdot 10^{+1}}$	$1.0 \cdot 10^{+2}$	$8.2 \cdot 10^{+2}$	$1.0 \cdot 10^{+4}$
($V_{m,k}$ / $V_{m,p}$)	$6.0 \cdot 10^{-6}$	$\mathbf{9.2 \cdot 10^{-2}}$	$1.0 \cdot 10^{-1}$	$8.2 \cdot 10^{-1}$	$1.0 \cdot 10^{+1}$
Nonlinear Fit	$\beta_{mk}(T) = \beta_{mk,0}\, e^{\alpha(T-T_r)}$		$\beta_{mk,0}$ = 0.274048 α = -2.487 T_r = 314.704		

Conclusions

The present paper examines the nonlinear dynamics of the heat-shock response in eukaryotic cells and performs a bifurcation analysis with respect to a key parameter ($\beta_{m,k}$), based on a nonlinear ODE model with many bilinear terms (which, albeit seemingly innocuous, has infinite equilibria). Certain steady states and nonlinear dynamics are explored; others can be found via homotopy continuation methods. The critical value $\boldsymbol{\beta^*_{m,k} = 9.2 \cdot 10^{+1}}$ induces a transition from proportional to saturated, extreme free HSP (x_{11}) response; $\boldsymbol{\beta^\dagger_{m,k} = 1.0 \cdot 10^{-1}}$ maximizes HSP transcription rate (x_5). Future goals include the explicit simultaneous integration of the system model and all (13·27=351) sensitivity ODEs to explore possible bifurcations due to other parameters, as well as the study of model-based robust control realizations (Khammash & El-Samad, 2004; El-Samad et al., 2005).

References

Allgower, E.L., Georg, K. (1990). *Computational Solution of Nonlinear Systems of Equations*, SIAM-AMS, USA.

Creagh, E.M., Sheehan, D., Cotter, T.G. (2000). Heat shock proteins – modulators of apoptosis in tumour cells. *Leukemia*, **14**, 1161-1173.

Dhooge, A., Govaerts, W., Kuznetsov, Y.A. (2003). MATCONT: A MATLAB package for numerical bifurcation analysis of ODEs. *ACM T. Math. Software*, **29**(2), 141-164.

El-Samad, H., Kurata, H., Doyle, J.C., Gross, C.A., Khammash, M. (2005). Surviving heat shock: Control strategies for robustness and performance. *PNAS*, **102**(8), 2736-2741.

Khammash, M., El-Samad, H. (2004). Systems biology: From physiology to gene regulation. *IEEE Contr. Syst. Mag.* **24**(4), 62-76.

Kline, M.P., Morimoto, R.I., (1997). Repression of the Heat Shock Factor 1 transcriptional activation domain is modulated by constitutive phosphorylation. *Mol. Cell. Biol.*, **17**(4), 2107-2115.

Lindquist, S. (1986). The heat-shock response. *Ann. Rev. Biochem.*, **55**, 1151-1191.

Meriin, A.B., Sherman, M.Y. (2005). Role of molecular chaperones in neurodegenerative disorders. *Int. J. Hyperther.*, **21**(5), 403-419.

Muchowski, P.J., Wacker, J.L. (2005). Modulation of neurodegeneration by molecular chaperones. *Nat. Neurosci.*, **6**(1), 11-22.

Morimoto, R.I. (1993). Cells in stress: Transcriptional activation of heat-shock genes. *Science*, **259**, 1409-1410.

Petre, I., Mizera, A., Hyder, C., Mikhailov, A., Eriksson, J., Sistonen, L., Back, R.-J. (2008). A new mathematical model for the heat shock response. In: Kok, J. (ed.), *Algorithmic Bioprocesses*, Springer Natural Computing.

Rieger, T.R., Morimoto, R.I., Hatzimanikatis, V. (2005). Mathematical modeling of the eukaryotic heat-shock response: Dynamics of the *hsp-70* promoter. *Biophys. J.*, **88**(3), 1646-1658.

Seydel, R. (1994). *Practical Bifurcation and Stability Analysis – From Equilibrium to Chaos*, Springer, USA.

Szilágyi, A., Kardos, J., Osváth, S. et al. (2007), Protein Folding, in: *Handbook of Neurochemistry and Molecular Neurobiology* (A. Lajtha, N. Banik, eds), Springer, USA.